

Original Article

A Rhodamine B Based Fe³⁺-Selective Colorimetric and Fluorescent Probe

Huang Yuxuan¹, Du Tengyuan², Yu Chunwei, Zhang Jun³

^{1,2,3}The NHC Key Laboratory of Tropical Disease Control, School of Life Sciences and Medical Technology, Hainan Medical University, Haikou, Hainan, China.

³Corresponding Author : jzhang@muhn.edu.cn (J. Zhang)

Received: 16 February 2026

Revised: 25 March 2026

Accepted: 11 April 2026

Published: 29 April 2026

Abstract - A novel rhodamine B-based derivative 1, functionalized with an Ethylenediamine-N-Ethanolamine moiety, was rationally designed and synthesized as an “off-on” fluorescent probe for Fe³⁺ detection. This probe demonstrated outstanding selectivity and high sensitivity toward Fe³⁺ over other competing metal ions in aqueous media, achieving a remarkably low detection limit of 0.33 μM. The sensing mechanism was attributed to a Fe³⁺-triggered, reversible ring-opening process of the Rhodamine Spirolactam Unit (RSL), which switched the fluorescence from a non-emissive state to a strongly emissive form. Based on Job’s plot analysis and spectroscopic titrations, a 1:1 binding stoichiometry between probe 1 and Fe³⁺ was established. Importantly, the practical utility of this probe was successfully validated through its application in the fluorescence imaging of Fe³⁺ in living cells, highlighting its potential for biological and environmental monitoring.

Keywords - Rhodamine B Derivative, Fluorescent Probes, Fe³⁺, Fluorescence Imaging, Off-On Signal.

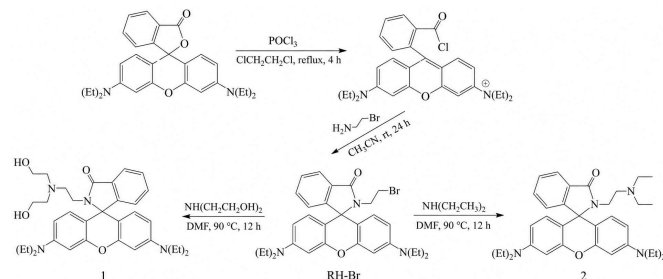
1. Introduction

In recent years, the development of artificial fluorescent probes for detecting environmentally and biologically significant ionic species, especially Heavy Transition-Metal (HTM) ions, has attracted substantial research interest [1-3]. Among these ions, Fe³⁺ plays an indispensable role in numerous biochemical processes, including oxygen transport, cellular metabolism, and electron-transfer systems. However, maintaining its homeostasis is critical, as both deficiency and excess of Fe³⁺ are associated with serious pathological conditions, such as neurodegenerative disorders (e.g., Parkinson’s and Alzheimer’s diseases) and oxidative stress-induced cellular damage [4,5]. Consequently, the ability to accurately, selectively, and conveniently monitor Fe³⁺ levels in physiological and environmental settings remains a pressing need. Despite this need, the design of highly selective “turn-on” fluorescent probes for Fe³⁺ presents a unique challenge. Unlike many other metal ions, paramagnetic Fe³⁺ is a potent fluorescence quencher due to its efficient spin-orbit coupling, which typically leads to fluorescence quenching (“turn-off”) rather than enhancement [6-11]. As a result, reported Fe³⁺ probes that operate via a fluorescence enhancement mechanism with high selectivity over competing HTM ions are exceptionally scarce. Most existing systems suffer from interference from other biologically relevant metals such as Cu²⁺, Hg²⁺, or Cr³⁺, or require complex experimental conditions, limiting their practical application. To overcome this limitation, a promising strategy involves

exploiting Chelation-Enhanced Fluorescence (CHEF) within a carefully designed molecular scaffold. This approach requires an intelligent integration of a fluorogenic unit with a receptor moiety tailored to the coordination geometry and ionic radius of Fe³⁺. The research is thus detailed: there is a critical demand for novel probe architectures that can not only overcome the inherent quenching nature of Fe³⁺ but also achieve high selectivity and sensitivity in aqueous or physiological media through a distinct “off-on” signaling mechanism. Guided by this rationale, a new rhodamine-based fluorescent probe for Fe³⁺ was designed and synthesized. The design is based on two key considerations: 1) Signal Transduction: rhodamine dye as an ideal fluorogenic platform was selected due to its excellent photophysical properties, including long excitation/emission wavelengths, high molar absorptivity, and quantum yield. Crucially, rhodamine derivatives exist in an equilibrium between a non-fluorescent spirocyclic (closed) form and a highly fluorescent ring-open form. Metal binding can trigger this structural switch, providing a built-in “off-on” fluorescence response [15]. 2) Receptor Design: Inspired by natural Fe³⁺-chelating siderophores (e.g., ferrichrome analogues), an Ethylenediamine-N-Ethanolamine moiety onto the rhodamine B core was incorporated. This flexible tripodal-like unit is designed to optimally accommodate Fe³⁺ through coordination with the amide oxygen, hydroxyl oxygen, and amine nitrogen atoms, promoting ring-opening and fluorescence turn-on upon complexation. This work aims to



address the identified gap by developing a selective and sensitive “turn-on” probe that operates via a CHEF mechanism, effectively countering the intrinsic quenching behavior of Fe^{3+} . The synthesis of the target probe is outlined in Scheme 1.



Scheme 1: Synthesis route of probe 1

2. Experimental Section

2.1. Apparatus and Reagents

Nuclear Magnetic Resonance (NMR) spectra were measured with a Bruker AVIII-500 spectrometer, and chemical shifts were given in ppm from Tetramethylsilane. Mass Spectra (MS) were recorded on a Thermo TSQ Quantum Mass Spectrometer. Fluorescence emission spectra were conducted on a HORIBA Fluoromax-4 spectrofluorometer. Absorption spectra were determined on a Beckman DU-800 spectrophotometer. The pH measurements were carried out on a PHS-3C meter. Elemental analysis was performed with a Vario III elemental analyzer.

Doubly distilled water was used throughout the experiments. All the materials for synthesis were purchased from commercial suppliers and used without further purification.

2.2. General Procedure for Spectroscopic Measurements

A stock solution of 1 (1 mM) was prepared in DMSO. To 5 mL glass tubes, 25 μL 1 (1 mM) and a proper amount of Fe^{3+} stock solution (1 mM) were added subsequently and then diluted with ethanol/HEPES buffer (8:2, v/v, pH 7.0, 50 mM). The resulting solution was mixed thoroughly. For all measurements, excitation and emission slit widths were 2 nm and 2 nm, respectively, and the excitation wavelength was 520 nm.

2.3. Cell Imaging

HeLa cells were kindly provided by Professor Yu Fabiao's research group. They were grown in 6-well coverslips and washed with Phosphate-Buffered Saline (PBS). Fe^{3+} (20 μM) (in PBS) was added to the cells and incubated for 30 min at 37 $^{\circ}\text{C}$, and then washed with PBS three times, followed by the addition of probe 1 (20 μM) and incubation for 30 min at 37 $^{\circ}\text{C}$. Fluorescence imaging in HeLa cells was recorded by a fluorescence microscope (Olympus FluoView Fv1000).

2.4. Synthesis of compounds 1 and 2

Compound RH-Br was synthesized according to the reported method.[16]

Compound 1: Under N_2 gas, compound RH-Br (494 mg, 0.90 mmol) and K_2CO_3 (500 mg, 3.62 mmol) were combined in DMF (10 mL) and stirred. Diethanolamine (0.45 mL, 4.5 mmol) in DMF (10 mL) was added dropwise. The reaction mixture was stirred at 90 $^{\circ}\text{C}$ for 12 h, filtered through Celite, and the solvent was evaporated under reduced pressure. Purification with silica gel Column Chromatography ($\text{CH}_2\text{Cl}_2/\text{acetic ether}=3:1$, v/v) afforded a pale pink solid. Yields: 360 mg (70 %). ^1H NMR (δ : ppm, CDCl_3): 7.88-7.91 (d, 1H, ArH), 7.44-7.45 (d, 1H, ArH), 7.43-7.44 (d, 1H, ArH), 7.06-7.08 (t, 1H, ArH), 6.50 (s, 1H, ArH), 6.48 (s, 1H, ArH), 6.38 (d, 2H, ArH), 6.30 (d, 1H, ArH), 6.28-6.29 (d, 1H, ArH), 4.15-4.17 (b, 2H, OH), 3.45-3.48 (t, 4H, CH_2), 3.31-3.36 (t, 8H, CH_2), 3.27-3.29 (t, 2H, CH_2), 1.15-1.18 (t, 12H, CH_3). ^{13}C NMR (δ : ppm, CDCl_3): 170.10 (C=O), 153.91, 153.27, 148.90, 132.69, 130.44, 128.51, 128.14, 123.80, 122.90, 108.24, 104.80, 97.79 (ArC), 65.87, 62.68, 44.66, 44.36, 12.60.

Compound 2 was synthesized following a similar procedure to that of compound 1 by the reaction of RH-Br with diethylamine. Purification with silica flash chromatography ($\text{CH}_2\text{Cl}_2/\text{acetic ether}=20:1$, $\text{CH}_2\text{Cl}_2/\text{acetic ether}=5:1$, v/v) affords 2 (75 %) as a pale pink solid. ^1H NMR (δ : ppm, CDCl_3): 7.80-7.82 (t, 1H, ArH), 7.31-7.32 (d, 2H, ArH), 6.95-6.96 (d, 1H, ArH), 6.36-6.38 (d, 2H, ArH), 6.30 (s, 2H, ArH), 6.16-6.18 (d, 2H, ArH), 3.62-3.65 (t, 2H, CH_2), 3.35-3.38 (t, 2H, CH_2), 3.21-3.26 (m, 8H, CH_2), 3.09 (t, 4H, CH_2), 1.05-1.08 (t, 12H, CH_3), 0.95 (t, 6H, CH_3). ^{13}C NMR (δ : ppm, CDCl_3): 168.38(C=O), 155.40, 153.99, 153.18, 148.82, 132.39, 130.68, 128.69, 127.90, 123.73, 122.79, 108.14, 105.49, 97.80 (ArC), 64.71, 61.91, 44.34, 41.53, 41.11, 39.

3. Results and Discussions

3.1. The Effect of Metal Ions on the Fluorescence and Absorption Spectra of Probe 1

The fluorescence and absorption spectra of probe 1 for metal ions and anions are shown in Figure 1. Compared to other metal ions and anions, the probe selectively recognized Fe^{3+} , emitting strong fluorescence at a wavelength of 587 nm, with a significant increase in fluorescence intensity (Figure 1a). Additionally, the ultraviolet-visible absorption spectroscopy experiments of probe 1 also demonstrated good selectivity for Fe^{3+} . The free probe 1 was colorless and showed little absorption at 556 nm. Notably, the addition of Fe^{3+} to the probe 1 solution caused a dramatic increase in the absorption peak at 556 nm, accompanied by a clear color change from colorless to pink. This indicated that probe 1 allowed for naked-eye detection of Fe^{3+} . The competition experiment, which was carried out by adding Fe^{3+} to 1 solution in the presence of other metal ions and anions, showed that the Fe^{3+} -induced fluorescent response was not interfered with by the

commonly coexisting ions. The result suggested that probe 1 showed a remarkable selectivity toward Fe^{3+} over other competitive ions (Figure 2).

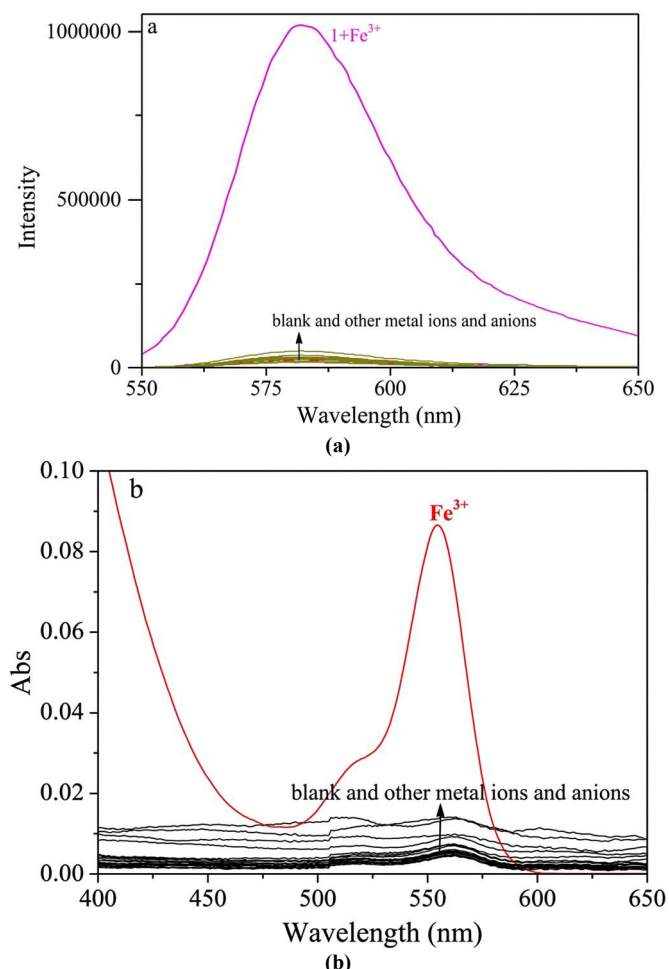


Fig. 1 (a) Fluorescent emission spectra of 1 (5 μM) to different metal ions and anions (50 μM) in aqueous ethanol (2:8, v/v) at pH 7.0; b) The absorption spectra of 1 (10 μM) with different metal ions and anions (50 μM) in aqueous ethanol (2:8, v/v) at pH 7.0.

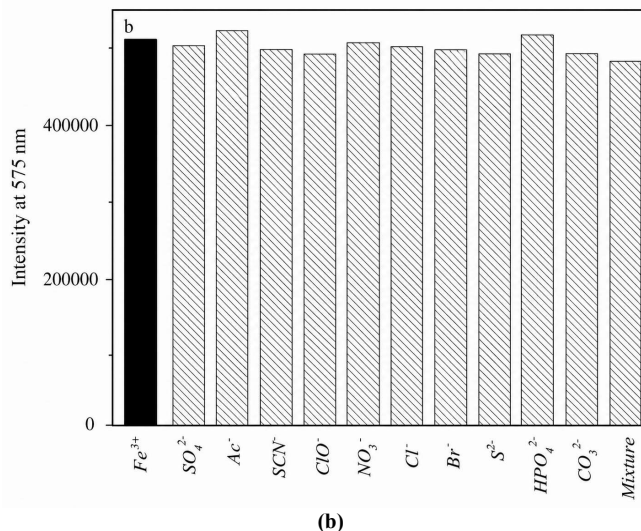
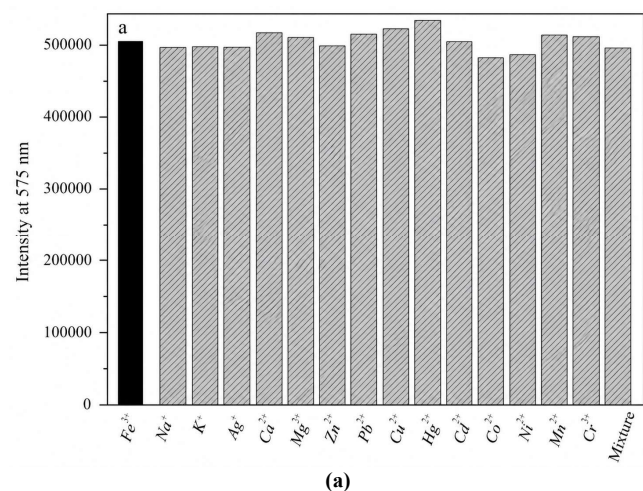
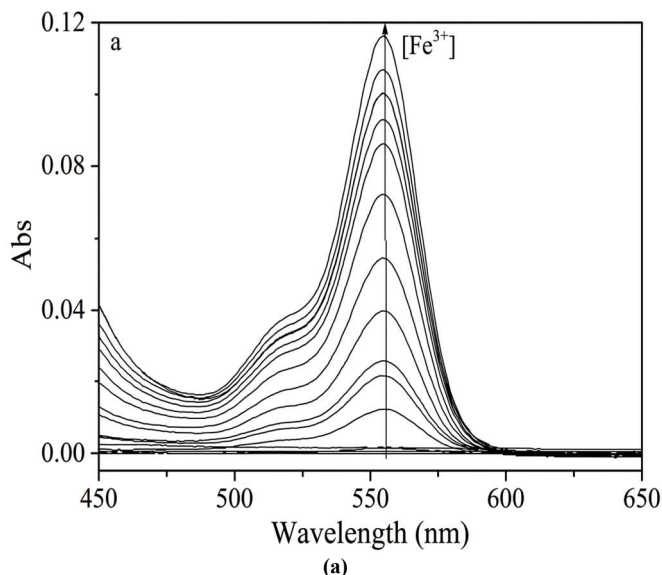


Fig. 2 (a) Fluorescence response of 1 (5 μM) to 10 μM of Fe^{3+} and to the mixture of 50 μM individual other metal ions with 10 μM of Fe^{3+} in aqueous ethanol (2:8, v/v) at pH 7.0; b) fluorescence response of 1 (5 μM) to 10 μM of Fe^{3+} and the mixture of 50 μM individual anions with 10 μM of Fe^{3+} in aqueous ethanol (2:8, v/v) at pH 7.0.

3.2. The effect of Fe^{3+} on the Fluorescence and Absorption Spectra of Probe 1

Further investigation of the effect of different concentrations of Fe^{3+} on the spectra of probe 1 is shown in Figure 3. The results indicated that before the addition of Fe^{3+} , the probe exhibited neither significant absorption peaks nor notable emission peaks in the 400-600 nm range. However, with the continuous increase in the concentration of Fe^{3+} , strong absorption and emission peaks appeared at 556 nm and 587 nm, respectively, and the color of the solution changed to pink. The fluorescence titration experiments demonstrated that detection of Fe^{3+} can be performed at the micromolar level of 0.33 μM when the concentration of the probe was 5 μM .



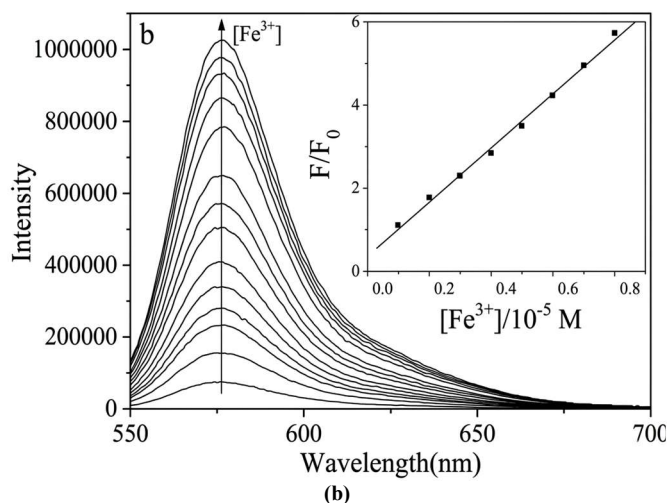


Fig. 3 (a) Absorbance spectra of 1 (10 μM) in the presence of different amounts of Fe^{3+} (0-100.0 μM) in aqueous ethanol (2:8, v/v) at pH 7.0. (b) Emission spectra of 1 (5 μM) in the presence of various concentrations of Fe^{3+} (0-50 μM) in aqueous ethanol (2:8, v/v) at pH 7.0. Inset: Linear fluorescence intensity (F/F_0) of 1 (5 μM) upon addition of Fe^{3+} (1-8 μM).

3.3. Discussion on the Mechanism of Probe 1 in Recognizing Fe^{3+}

The 1:1 binding mode was supported by Job's plot (Figure 4). The addition of Ethylenediamine to the mixture of compound 1 (5 μM) and Fe^{3+} (50 μM) decreased the fluorescence intensity of the solution (Figure 5), and the color of the mixture changed back to colorless. Upon re-adding Fe^{3+} , the signal intensity was restored, which implied reversible binding between compound 1 and Fe^{3+} . To further validate the performance of the control compound 2, it was found that there was no significant recognition ability for common metal ions. This indicated that the Hydroxyl oxygen atom in the recognition unit of compound 1 was involved in coordination with Fe^{3+} , further confirming our design concept.

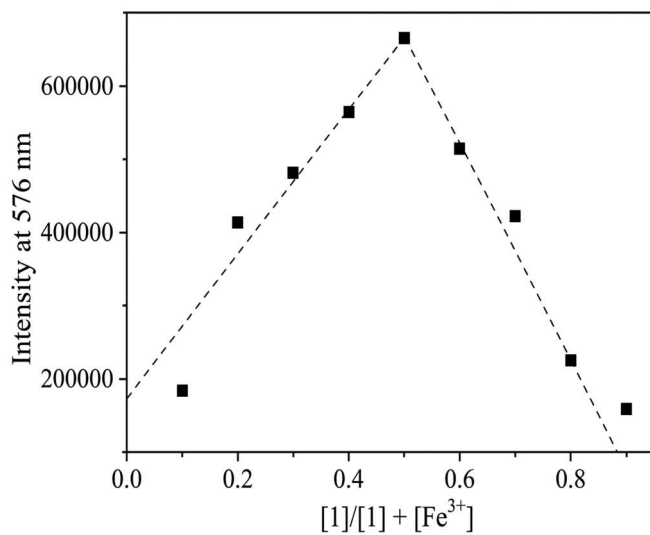


Fig. 4 Job's plot of 1 with Fe^{3+} . The total concentration of 1 and Fe^{3+} was kept at a fixed 20 μM .

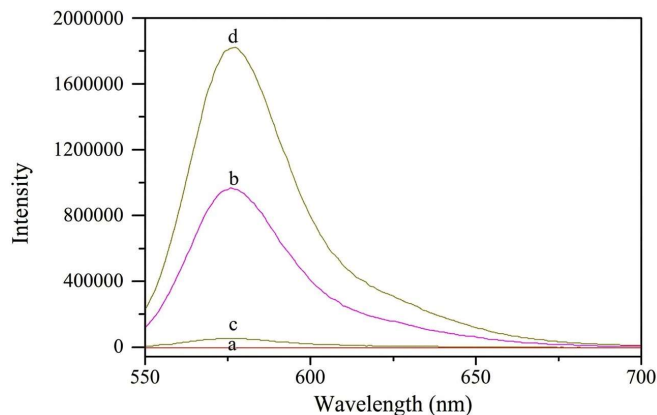


Fig. 5 Reversible titration response of 1 to Fe^{3+} in aqueous ethanol (2:8, v/v) at pH 7.0. (a) 1 (5 μM); (b) 1 (5 μM) with Fe^{3+} (50 μM); (c) 1 (5 μM) with Fe^{3+} (50 μM) and then addition of EDA (100 μM); (d) 1 (5 μM) with Fe^{3+} (50 μM) and EDA (100 μM) and then addition of 100 μM Fe^{3+} .

3.4. Bioimaging Application

A practical bioimaging application of 1 for Fe^{3+} in biological samples was developed by confocal fluorescence microscopy on an Olympus FluoView FV1000 laser scanning microscope. When excited by 520 nm light, staining HeLa cells with a 20 μM solution of 1 for 30 min at 37 $^{\circ}\text{C}$ led to very weak intracellular fluorescence (Figure 6a). The cells were then supplemented with 20 μM Fe^{3+} in the growth medium for 30 min at 37 $^{\circ}\text{C}$ and loaded with 1 under the same conditions; a significant increase in the fluorescence from the intracellular area was observed (Figure 6b). Bright-field measurements confirmed that the cells after treatment with Fe^{3+} and 1 were viable throughout the imaging experiments (Figure 6c, Figure 6d).

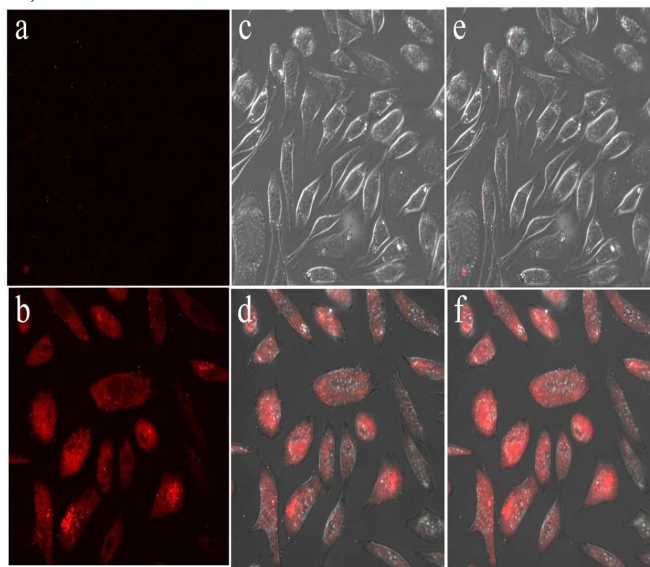


Fig. 6 Confocal fluorescence and bright field images of HeLa cells. (a) cells stained with 20 μM 1 for 30 min at 37 $^{\circ}\text{C}$; (b) cells supplemented with 20 μM FeCl_3 in the growth media for 30 min at 37 $^{\circ}\text{C}$ and then incubated with 20 μM 1 for 30 min at 37 $^{\circ}\text{C}$; (c) bright field image of cells shown in panel (a); (d) bright field image of cells shown in panel (b); (e) overlap image of panel (a); (f) overlap image of panel (f) ($\lambda_{\text{ex}} = 559 \text{ nm}$)

4. Conclusion

In conclusion, 1 was an “off-on” type probe for Fe³⁺, which exhibited excellent selectivity over other metal ions and anions. Moreover, probe 1 can be used for monitoring intracellular Fe³⁺ levels in living cells.

Conflicts of Interest

The authors declare that there is no conflict of interest regarding the publication of this paper.

Funding Statement

This work was financially supported by the Undergraduate Research and Innovation Training Program of Hainan Medical University (No. RZ2500002218), the Academic Enhancement Support Program of Hainan Medical University (No. XSTS2025127, No. XSTS2025192), and the Research and Training Foundation of China (No. S202511810047).

References

- [1] Ksenia V. Ksenofontova et al., “Amine-Reactive BODIPY Dye: Spectral Properties and Application for Protein Labeling,” *Molecules*, vol. 27, no. 22, pp. 1-20, 2022. [[CrossRef](#)] [[Google Scholar](#)] [[Publisher Link](#)]
- [2] Riya Choudhary, and Sachin Kumar Srivastava, “Templating Assisted Fabrication of Flexible, Highly Stable and Uniform Plasmonic Platform for Ultrahigh Enhancement of Raman and Fluorescence Signals: Model Sensing of Rhodamine-6G,” *Spectrochimica Acta Part A: Molecular and Biomolecular Spectroscopy*, vol. 338, 2025. [[CrossRef](#)] [[Google Scholar](#)] [[Publisher Link](#)]
- [3] Dongsheng Xiang et al., “A Novel on-off Fluorescent Probe with Rapid Response for the Selective and Sensitive Detection of Co²⁺,” *Inorganic Chemistry Communications*, vol. 111, 2020. [[CrossRef](#)] [[Google Scholar](#)] [[Publisher Link](#)]
- [4] James P. Sumnera, and Raoul Kopelman, “Alexa Fluor 488 as an Iron Sensing Molecule and its Application in PEBBLE Nanosensors,” *Analyst*, vol. 130, no. 4, pp. 528-533, 2005. [[CrossRef](#)] [[Google Scholar](#)] [[Publisher Link](#)]
- [5] Philip Aisen, Marianne Wessling-Resnick, and Elizabeth A Leibold, “Iron Metabolism,” *Current Opinion in Chemical Biology*, vol. 3, no. 2, pp. 200-206, 1999. [[CrossRef](#)] [[Google Scholar](#)] [[Publisher Link](#)]
- [6] Bao-xing Shen, and Ying Qian, “Building Rhodamine-BODIPY Fluorescent Platform using Click Reaction: Naked-Eye Visible and Multi-Channel Chemodosimeter for Detection of Fe³⁺ and Hg²⁺,” *Sensors and Actuators B: Chemical*, vol. 260, pp. 666-675, 2018. [[CrossRef](#)] [[Google Scholar](#)] [[Publisher Link](#)]
- [7] Jie Zhang et al., “Novel Fluorescent Probe Toward Fe³⁺ based on Rhodamine 6G Derivatives and its Bioimaging in Adult Mice, *Caenorhabditis Elegans*, and Plant Tissues,” *ACS Omega*, vol. 6, no. 12, pp. 8616-8624, 2021. [[CrossRef](#)] [[Google Scholar](#)] [[Publisher Link](#)]
- [8] K.M. Alotaibi et al., “Total Determination and Chemical Speciation of Fe²⁺ and Fe³⁺ Species in Water based on the Fluorescence Quenching of 4,5-dihydroxy-1,3-Benzenedisulfonic Acid as a Sensing Platform,” *Journal of Fluorescence*, vol. 35, no. 12, pp. 13103-13115, 2025. [[CrossRef](#)] [[Google Scholar](#)] [[Publisher Link](#)]
- [9] Md Foridul Islam et al., “A Rhodamine B-based “Turn-On” Fluorescent Probe for Selective Fe³⁺ Ions Detection,” *Sensors*, vol. 25, no. 11, pp. 1-15, 2025. [[CrossRef](#)] [[Google Scholar](#)] [[Publisher Link](#)]
- [10] Xin Jiang et al., “A Ratiometric Fluorescent Probe based on RhB Functionalized Tb-MOFs for the Continuous Visual Detection of Fe³⁺ and AA,” *Molecules*, vol. 28, no. 15, pp. 1-14, 2023. [[CrossRef](#)] [[Google Scholar](#)] [[Publisher Link](#)]
- [11] Rupinder Singh et al., “Al³⁺ Sensing through Different Turn-on Emission Signals vis-a-vis Two Different Excitations: Applications in Biological and Environmental Realms,” *Analytica Chimica Acta*, vol. 1025, pp. 172-180, 2018. [[CrossRef](#)] [[Google Scholar](#)] [[Publisher Link](#)]
- [12] Gasser M. Khairy et al., “Fluorescence Determination of Fe (III) in Drinking Water using a New Fluorescence Chemosensor,” *RSC Advances*, vol. 12, no. 42, pp. 27679-27686, 2022. [[CrossRef](#)] [[Google Scholar](#)] [[Publisher Link](#)]
- [13] Amal Al-Azmi, and Elizabeth John, “Synthesis and Characterization of Novel Tricyanofuran Hydrazone Probe: Solvatochromism, Density-Functional Theory Calculation and Selective Fluorescence, and Colorimetric Determination of Iron (III),” *Luminescence*, vol. 36, no. 5, pp. 1220-1230, 2021. [[CrossRef](#)] [[Google Scholar](#)] [[Publisher Link](#)]
- [14] Li Xiao et al., “Reaction-based Fluorescent Silk Probes with High Sensitivity and Selectivity to Hg²⁺ and Ag⁺ Ions,” *Journal of Material Chemistry C*, vol. 9, no. 14, pp. 4877-4887, 2021. [[CrossRef](#)] [[Google Scholar](#)] [[Publisher Link](#)]
- [15] Yuqi Zhang et al., “A Novel Rhodamine-based Colorimetric and Fluorometric Probe for Simultaneous Detection of Multi-Metal Ions,” *Spectrochimica Acta Part A: Molecular and Biomolecular Spectroscopy*, vol. 230, 2020. [[CrossRef](#)] [[Google Scholar](#)] [[Publisher Link](#)]
- [16] Yasuhiro Shiraishi et al., “A Rhodamine-Cyclen Conjugate as a Highly Sensitive and Selective Fluorescent Chemosensor for Hg (II),” *Journal of Organic Chemistry*, vol. 73, no. 21, pp. 8571-8574, 2008. [[CrossRef](#)] [[Google Scholar](#)] [[Publisher Link](#)]